SOURCE AND PATH CALIBRATION IN REGIONS OF POOR CRUSTAL PROPAGATION USING TEMPORARY, LARGE-APERTURE, HIGH-RESOLUTION SEISMIC ARRAYS

John L. Nabelek[1], Seth Carpenter[1], Patrick W. Monigle[1], Jochen Braunmiller[1], and W. Scott Phillips[2]

Oregon State University[1] and Los Alamos National Laboratory[2]

Sponsored by Air Force Research Laboratory and the National Nuclear Security Administration

Contract No. FA8718-09-C-0004
Proposal No. BAA09-28

ABSTRACT

Broadband seismic data acquired during the Hi-CLIMB experiment are used to study seismic events and path propagation in the Nepal Himalaya and the south-central Tibetan Plateau. The 2002–2005 experiment consisted of 233 stations along a dense 800 km linear north-south array extending from the Himalayan foreland into the central Tibetan Plateau. The main array was flanked by a 350 km x 350 km sub-array in southern Tibet and central and eastern Nepal. The dataset provides an opportunity to obtain seismic event locations for ground truth (GT) evaluation, to determine source parameters, and to study distance evolution of seismic coda for yield estimation in low Q regions.

In year two of the project we concentrated on refining hypocenter locations and magnitude estimates in Tibet near the Hi-CLIMB stations. Better event locations are primarily due to improvements in crustal models and to eliminating spurious events and arrivals. The dataset now holds over 34,000 events with ~8,900 defined by more than 30 phase arrivals, which we consider well located. In southern Tibet, many well-located earthquakes occur in the lower crust and upper mantle. Abundant seismicity north of the Yarlung Tsangpo Suture, however, occurs primarily in the upper-most crust in extensional grabens and along strike-slip faults connecting them. Many initial event magnitudes were contaminated by arrivals from closely following, larger events during times of vigorous seismicity. Use of vertical component data consistently underestimates the S arrival amplitude, which led to systematically underestimated magnitudes. Using only P-arrivals eliminated contamination and provided a much cleaner magnitude dataset, which can be uniformly converted to S-based magnitude by adding a constant 0.7 to compensate for the average S-to-P amplitude ratio for earthquakes with double-couple mechanisms. This corrected P-derived M_L is consistent with M_w from low-frequency regional moment tensor analysis we have performed on larger events in our dataset.

In-depth analysis focused on seismicity along the Pumqu-Xianza Rift (PQX) (~30ºN, 88ºE) an area of known geothermal activity and exceptionally high rate of seismicity. Hi-CLIMB stations operating in the region from July 2004 to August 2005 recorded over 500 well-located earthquakes near the PQX compared to only 11 events listed in the USGS NEIC catalog for the same region. The USGS locations show a systematic west-southwest bias of up to ~40 km compared to locations based on automatic P- and S-phase picks from local stations, which are tightly clustered and ~20 km west of the central PQX. Epicenters from manual phase picking differ by only a few km from the automatic locations confirming their overall quality. Manually derived hypocenter depths of ~10 km are consistent with regional moment tensor depths of 36 larger ($3.5 \leq M_w \leq 4.8$) earthquakes recorded by Hi-CLIMB. All source mechanisms show ~N-S oriented normal faulting with a shallow west-dipping nodal plane. Based on event locations, source mechanisms, and Google imagery showing no prominent scarps in the immediate vicinity of the earthquakes, we favor a scenario of rupture along the eastern PQX rift boundary fault, a west-dipping low-angle normal fault and the most prominent feature on the Google imagery.

OBJECTIVES

The broadband dataset from the 2002–2005 Hi-CLIMB seismic array in the Himalayan-Tibetan collision zone is unique in its large aperture and dense station spacing. The purpose of our research is to improve source and path calibration in regions of poor crustal propagation to enhance the monitoring community's capabilities to estimate magnitude and yield of future nuclear tests in low Q and highly scattering environments. We have three linked objectives. The first is to obtain high-precision ground-truth seismic event hypocenters. The second is to provide seismic moment and independent depth estimates from waveform modeling of local and regional earthquakes. The third is to determine the distance evolution of seismic coda, utilizing the quasi-continuous control offered by the dense, laterally large network, important for low Q areas. In the second year of the project, efforts concentrated on (i) improving the seismic event database obtained from automatic phase picking and event association, (ii) improving consistency and reliability of the local magnitude estimates, and (iii) in-depth analysis for absolute event location and moment tensor analysis focusing initially on a small area, the Pumqu-Xianza rift in southern Tibet.

RESEARCH ACCOMPLISHED

Data

The Hi-CLIMB broadband seismic experiment (Nabelek et al., 2005; 2009a) in Nepal and the south-central Tibet consisted of 233 sites with each site occupied for 12-20 months (Figure 1). Station spacing along the ~800-km long north-south array covering the India-Eurasia collision zone from the Ganges foreland into the Tibetan Plateau was 3-4 km in the south and about 8 km north of the Yarlong-Tsangpo suture. Lateral deployments in Nepal and southern Tibet with 30-40 km station spacing improve earthquake location capabilities and provide wave propagation control for the transition from the foreland into the plateau. Data were recorded continuously at 50 and 40 sps. The Hi-CLIMB data provide a unique opportunity to study small sized seismic events at unprecedented accuracy in central Asia.

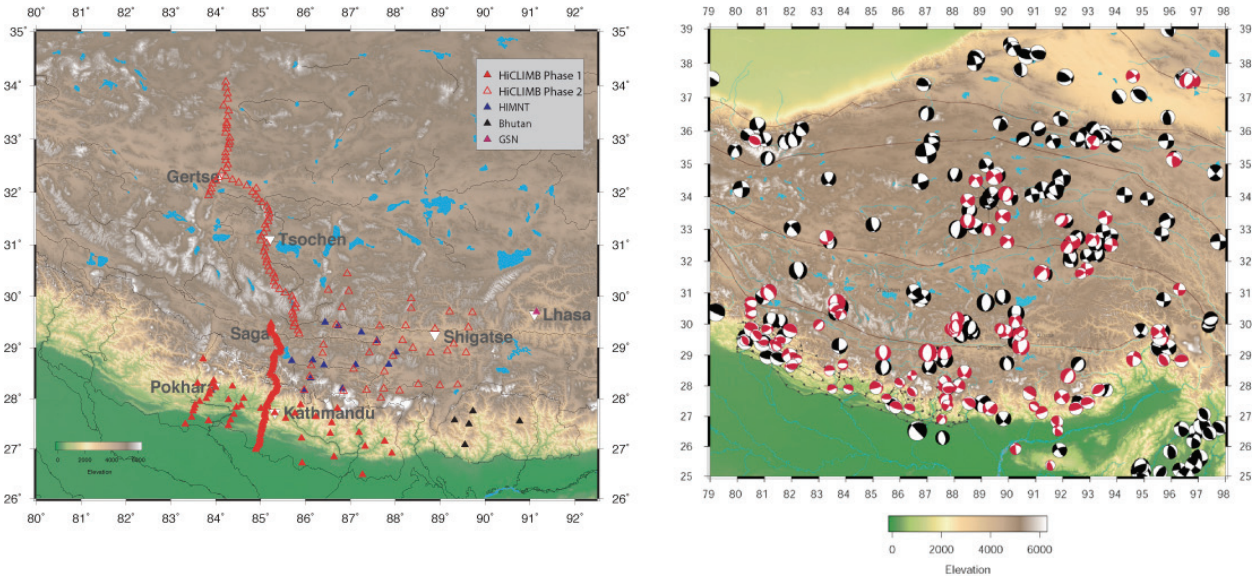

Figure 1. Left. Map of Hi-CLIMB (red triangles) 233 station seismic network, and HIMNT (blue triangles) (Sheehan et al., 2004) and Bhutan (black triangles) (Velasco et al., 2007) broadband temporary seismic networks also available for this study. Purple triangle: Permanent broadband station in Lhasa. Right. Regional moment tensors (red: Burtin, 2005; Baur, 2007; Monigle et al., 2009) and Global CMTs (black). We completed analysis of 170+ larger events in the Tibet region using high-quality waveforms. The 150+ Hi-CLIMB solutions contain events as small as M_w = 3.5. 166 CMTs, mainly for M_w>5.0, exist for 1976-2005.

We had already performed regional moment tensor analysis in the Himalayan-Tibetan region for ~150 selected larger earthquakes (Burtin, 2005; Burtin et al., 2005; Baur, 2007) using the full waveform inversion code of Nabelek and Xia (1995). Results (Figure 1, Nabelek et al., 2009b) illustrate that our efforts substantially expand the region's moment tensor catalog; our database also includes most events analyzed by de la Torre et al. (2007). Analysis suggests a depth resolution for shallow crustal events on the order of ±5 km and an estimated M_w uncertainty of ±0.1-0.2 units with currently used velocity models and event locations. Additional moment tensors were obtained for the Pumqu-Xianza Rift (~ 30ºN, 88ºE) (see below) where we have good event location control, a significant number of events with similar-looking waveforms spanning a wide size range, and good recording geometry that allows testing of parameter resolution and evaluating of velocity-depth models for seismogram calculation.

Event Detection and Location

In year two of the project we concentrated on refining hypocenter locations and magnitude estimates in Tibet near the Hi-CLIMB stations. The entire Hi-CLIMB waveform database (1.4 TB) has been organized using the Antelope software developed by Boulder Real Time Technologies (BRTT). We used the Antelope modules for automatic detection and arrival time picking, event-arrival association and event location. Requiring low detection (3.0 STA/LTA ratio) and association (7 and more phases constitute an event) thresholds implemented to obtain a dataset as complete as possible resulted in an initial database of almost 110,000 declared events for the second half of the experiment (15 months from June 2004 to August 2005) or on average ~240 per day.

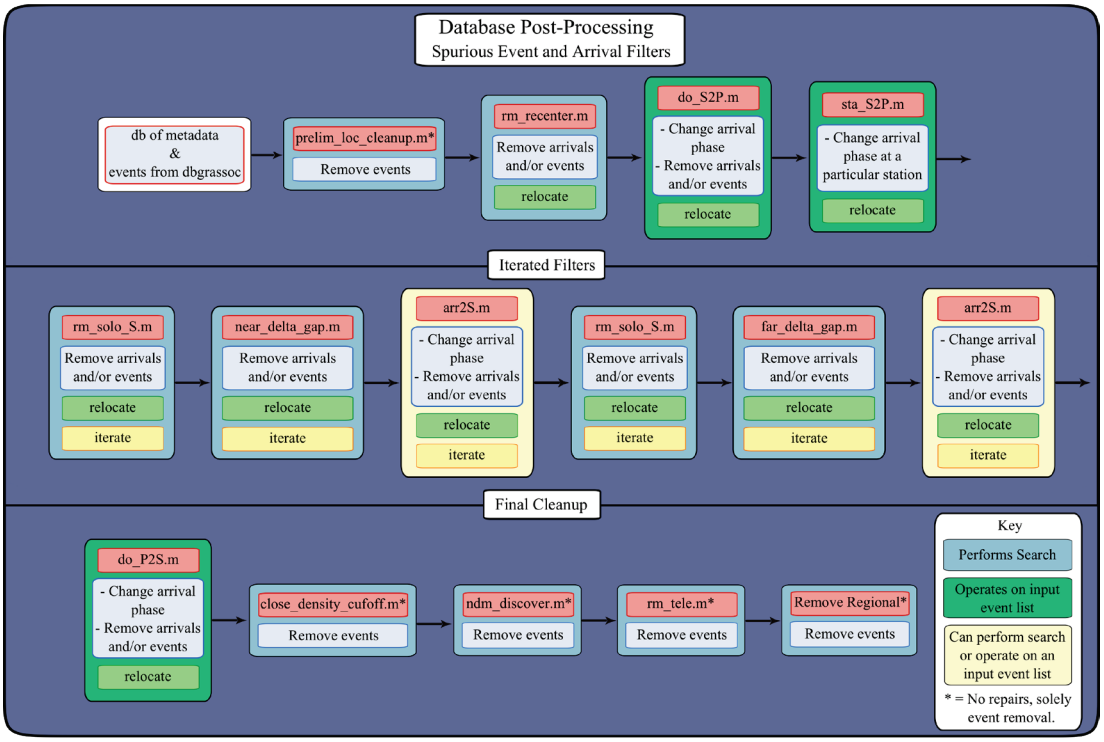

Figure 2. Simplified flowchart showing database post-processing steps performed to clean up the associated event table. Processing steps fall into two groups: (1) removing or reassigning phase picks to obtain a more consistent set of phase picks for an event leading to an improved location (green box "relocate") or (2) removing spurious events for which the set of phase picks could not be fixed (blue box "Remove events"). Details are described in Carpenter (2010).

The large number of events rendered manual inspection unfeasible and we spent considerable effort to develop modules to weed out spurious detections as well as erroneous phase and event associations to automate data management. Figure 2 shows a simplified flowchart of post-processing steps that implement simple logic considerations about what constitutes a valid seismic event. For example, we expect that stations close to an

epicenter record an event and that stations close to each other either all (or most) record an event or do not. Many problems stemmed from wrong phase association caused by simultaneously occurring events in different locations within the Hi-CLIMB array region, misplaced seismicity from the great 2004 Sumatra earthquake sequence or incorrectly associating P arrivals as S arrivals, or vice versa. We tested phase arrivals for each event and removed spurious arrivals or switched mis-associated arrivals (e.g., S- to P-phase) to improve the consistency of the phase-arrival set for an event; if this was impossible, we removed events entirely.

The resulting automatic preliminary event database contains more than 34,000 seismic events, with about 8,900 defined by more than 30 P and S arrivals. Figure 3 shows a subset of 4,500 well located events with at least 30 defining arrivals and local magnitude $M_L(P) \geq 2.0$, which is a relevant cut-off for monitoring purposes ($M_L(P)$ is defined below). The automatic locations utilize many S-arrivals, constraining the epicenters, and correlate with geologic structures seen in satellite imagery suggesting they are quite accurate; for some events the USGS PDE locations show a mismatch of up to 50 km (see Pumqu-Xianza section below for quantitative analysis of PDE and automatic location bias). Most shallow seismicity north of the Yarlung-Tsangpo suture (north of 29.5°N) is in an area not investigated by most other previous experiments. The most prolific source region was the Payang Basin (near 30º-31ºN, 84ºE), with almost 10,000 events following $M_w > 6$ main shocks in July 2004 and April 2005, respectively (Figure 4); the extreme number of events immediately after the main events actually was one of the primary reasons for phase misassignments requiring database post-processing (Figure 2). Vigorous seismicity (1,600+ events) was also observed from the vicinity of the Pumqu-Xianza Rift (~30ºN, 88ºE).

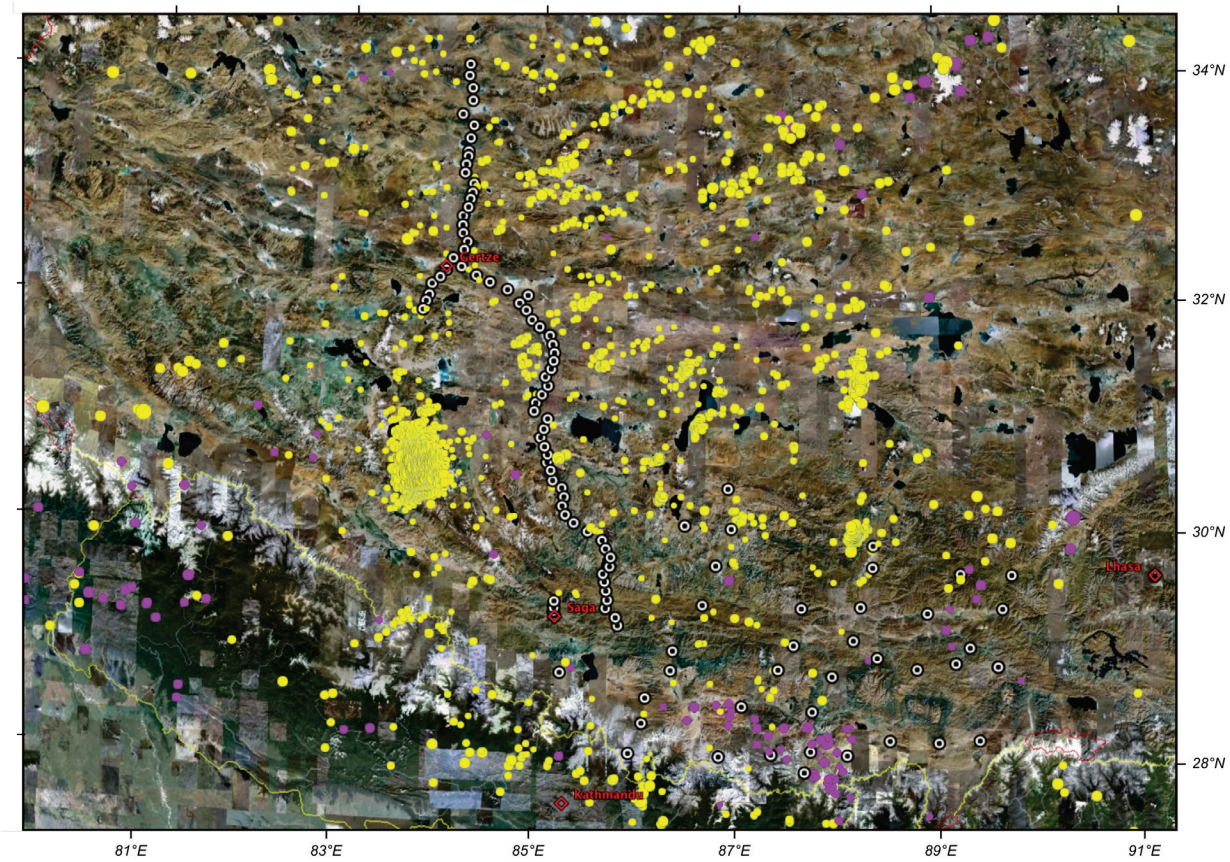

Figure 3. Preliminary epicenter map (colored circles) for 15-month period covering the second half of Hi-CLIMB (recording stations black circles). Over 34,000 events have been located. We plot 4,500 events with at least 30 P and S arrivals and $M_L(P) \geq 2.0$. Yellow are crustal events and purple are upper mantle events. The numerous shallow events north of the Yarlung-Tsangpo suture (>29°N) have not been covered by previous experiments.

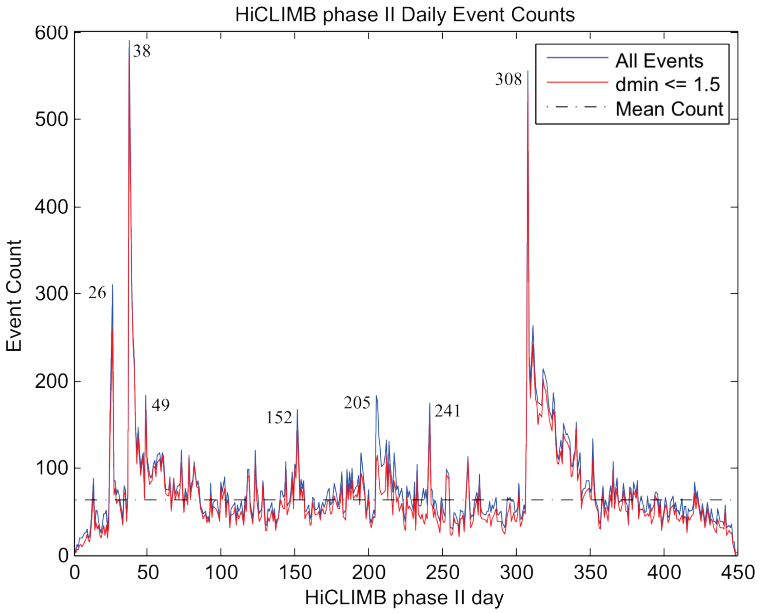

Figure 4. Events per day in the 34,000+ Hi-CLIMB phase II database (June 2004 – August 2005). Peaks at day 38 and 308 are immediate aftershocks of Payang Basin M 6+ main shocks. Day 26 and 49 peaks are partially due to elevated seismicity in the Pumqu-Xianza Rift. Red shows event counts with closest station 1.5° or less away from an event, blue are all events. The peak at day 205 is due to the 2004/12/26 M_w=9.1 Sumatra-Andaman earthquake about 20° SE from the array; its aftershocks were very well-recorded by the Hi-CLIMB array, however, automated processing encountered difficulties determining correct slowness and/or depth resulting in a significant number of events being mislocated inside or near the array requiring database post-processing (Figure 2).

Efforts will now concentrate on identifying potential GT5 events and to determine their locations based on manually picked phases with careful consideration on depth and absolute location uncertainties as required. This work will include improving crustal structural models. Selected small events near the dense array will be analyzed in conjunction with the GT location effort (e.g., to obtain independent depth estimates) and the requirements of the coda wave modeling (e.g., to provide seismic moment over a range of event sizes for calibration of absolute spectral levels from coda to bands approaching those used for yield estimation).

Local Magnitude

We used the Antelope module dbml to calculate local magnitude (M_L) from the vertical component seismograms for all events in the database with epicenter-station distances of 600 km or less. Usually M_L is determined from the maximum amplitudes on Wood-Anderson-equivalent horizontal seismograms with the maximum amplitude corresponding to an S-phase. We thus originally defined the time window to be 1.5 times the S-P-time for a given station-event distance to obtain the amplitudes. However, during times of vigorous seismicity, we often encountered contamination by arrivals from closely following, larger events (Figure 5). Another complication arises from using vertical component data that underestimate the S arrival amplitude, which led to systematically underestimated magnitudes.

In order to avoid both problems, we decided to estimate event size from a short time window containing only P waves (0.25 S-P-time, Figure 5). This approach eliminated contamination and provided a much cleaner magnitude dataset. Using the average expected S-to-P amplitude ratio of $(v_p/v_s)^3 \approx 5$ for earthquakes with a double-couple mechanism provides a physics-based approach to convert to S-based magnitude by simply adding a constant value of 0.7. We call this (corrected) magnitude M_L(P).

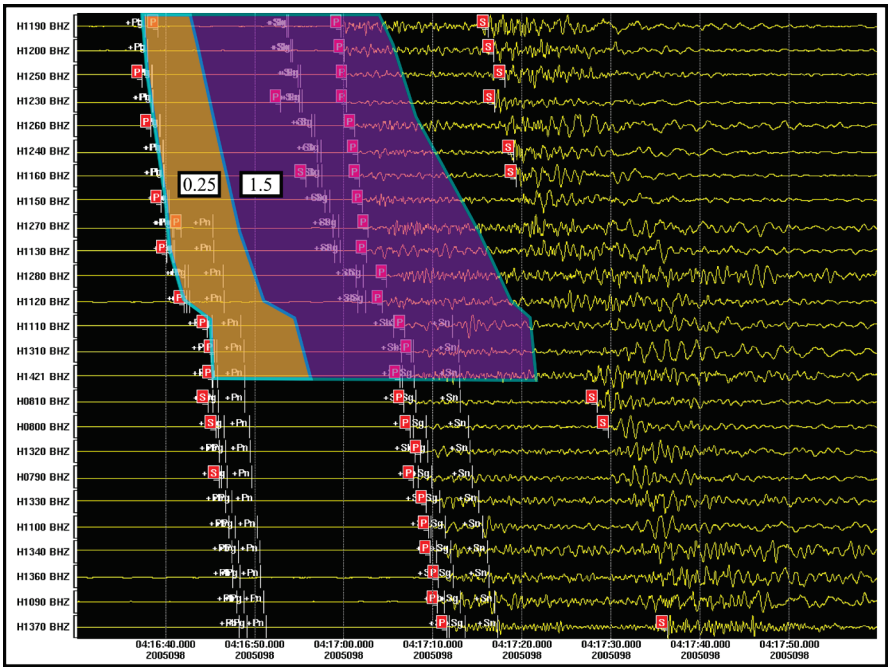

Figure 5. Wood-Anderson equivalent waveforms for 90 seconds of data from April 8, 2005, about 8 hours after an M=6+ earthquake in the Payang Basin. A small event (first set of arrivals) is followed by a much stronger event (second set of P arrivals) within 1.5 times its S-P-time (purple area). The M_L for the first event based on the long time window is about 2 magnitude units too large. Another problem, apparent for the second event, is that vertical seismograms underestimate the amplitude of S-phases, which are predominantly recorded on horizontal components; in this case the S-to-P amplitude ratio is about 2 compared to the expected value of ~5. We decided to determine magnitudes from a short window containing only the P arrival (0.25 S-P-time shown in brown).

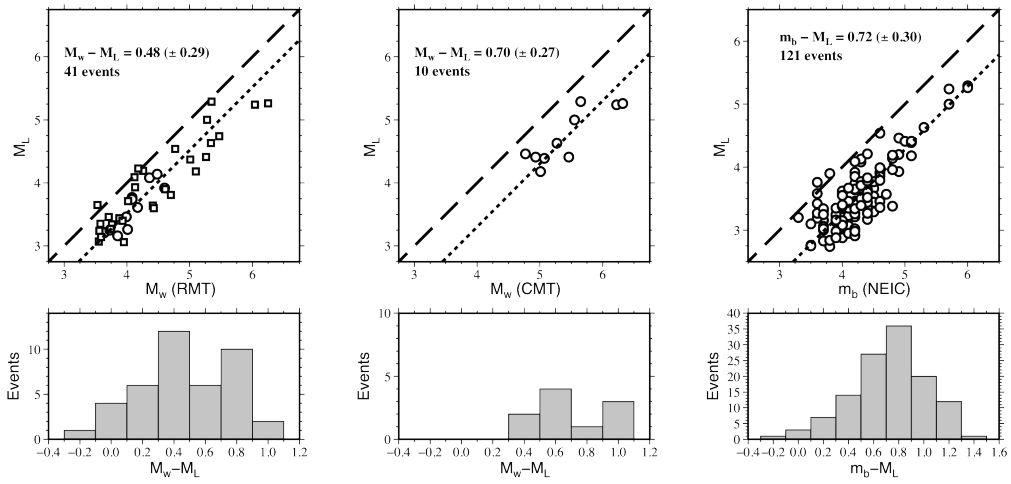

Figure 6. Magnitude comparison. M_L is local magnitude based on P wave amplitudes determined during automatic processing. M_w(RMT), M_w(CMT), m_b(NEIC) are moment magnitude from regional moment tensor inversion, Global CMT analysis, and USGS NEIC body wave magnitude, respectively. Shown are common events. The average underestimation of uncorrected M_L of 0.5, 0.7, and 0.7, respectively, is consistent with the expected theoretical bias due the use of P instead of S waves. The scatter around the average (short dashes, long dashes correspond to one-to-one correspondence) is similar to scatter observed when regressing other magnitudes relative to each other (e.g., Braunmiller et al., 2005).

We found our $M_L(P)$ (P-wave M_L + 0.7) is consistent with the moment magnitude M_w determined from low-frequency regional moment tensor analysis for 41 common events, the average $M_L(P)$-M_w(RMT) difference is 0.2 units (Figure 6). We also compared $M_L(P)$ with Global CMT M_w and USGS PDE body wave magnitude m_b, which for moderate event sizes is close to M_w. We found on average $M_L(P)$ matches exactly both teleseismic estimates (Figure 6).

Low-Angle Normal Faulting in the Pumqu-Xianza Rift

Seismicity north of the Yarlung-Tsangpo Suture in the Lhasa Terrane of southern Tibet occurs primarily along N-S trending grabens. In-depth analysis concentrated on particularly focused seismicity along the Pumqu-Xianza rift (PQX) (Figure 7) an area of known geothermal activity and exceptionally high rate of seismicity that initiated in 1980 following an M_S 6.2 earthquake in the northern part of the rift. Hi-CLIMB stations operating in the area from July 2004 to August 2005 recorded over 500 well-located earthquakes near the PQX rift compared to only 11 events, ranging in magnitude (m_b) from 4.0 to 4.8, listed in the USGS NEIC catalog.

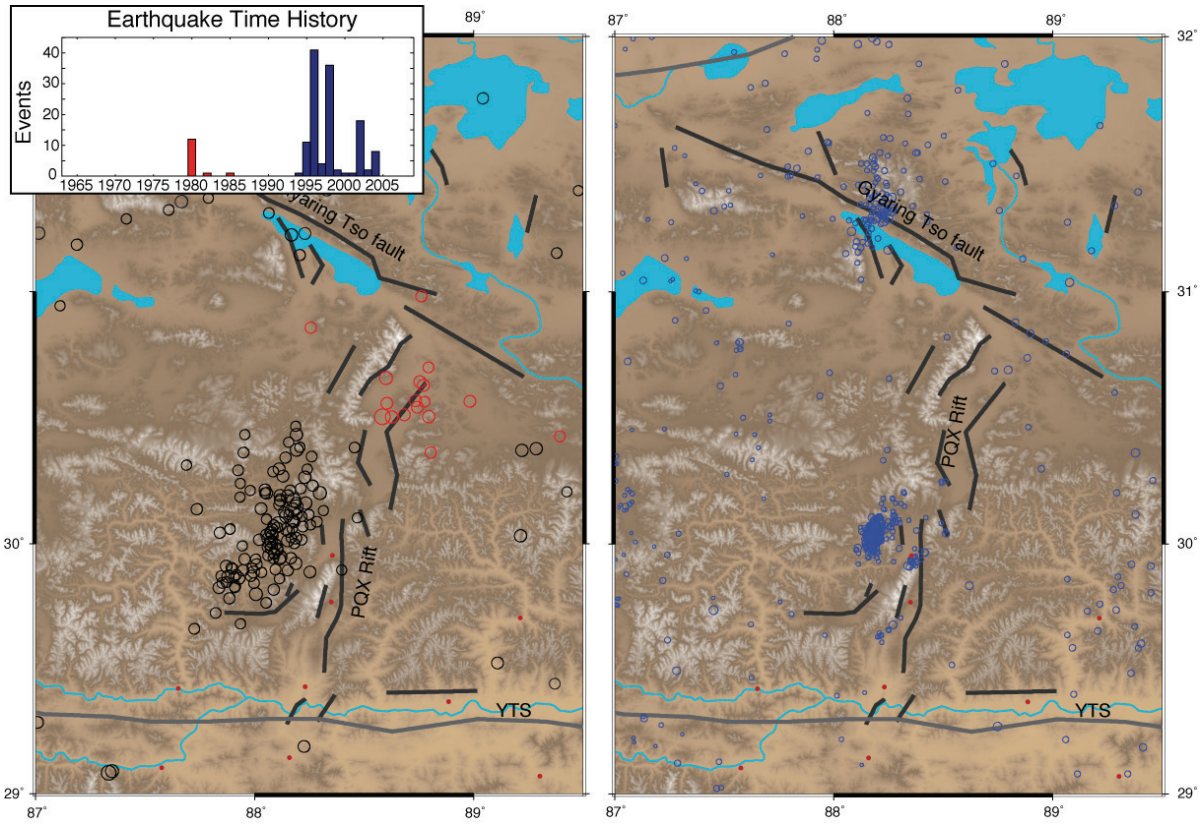

Figure 7. Left. Map and time history (inset) of 1963-2009 seismicity ($m_b \geq 4.0$). An M_S 6.2 event in 1980, the largest historic PQX event, initiated activity in the northern rift (red). After a ~10 year hiatus, activity started in the central part (black). Right. Hi-CLIMB seismicity. Shown are 500+ high-quality epicenters (blue) for events from July 2004 to August 2005, when close-by sites (red) operated, based on at least 20 automatic phase picks. Note tight event cluster at 30ºN about 20 km west of the graben.

Locations with local Hi-CLIMB stations reveal a systematic west-southwest bias of the routine NEIC epicenter locations that can reach up to ~50 km (Figure 8). The Hi-CLIMB locations based on automatic P- and S-phase pick are closer to the rift and cluster near the central PQX. Manual phase picking for selected events verified the high

automatic location quality with epicenter differences of only a few kilometers (Figure 8). Manual locations include a larger number of phase picks, in particular, many more S picks from close-by stations that provide strong epicenter and depth control. The resulting hypocenters cluster very tightly west of the central PQX (triangles in Figure 8) near ~10 km depth. The cluster technically does not satisfy GT5 criteria (e.g., Bondar et al., 2004), even though the closest site is ~20 km from the epicenters, because of the large ~150º azimuthal gap since the events occurred at the northern terminus of the lateral array.

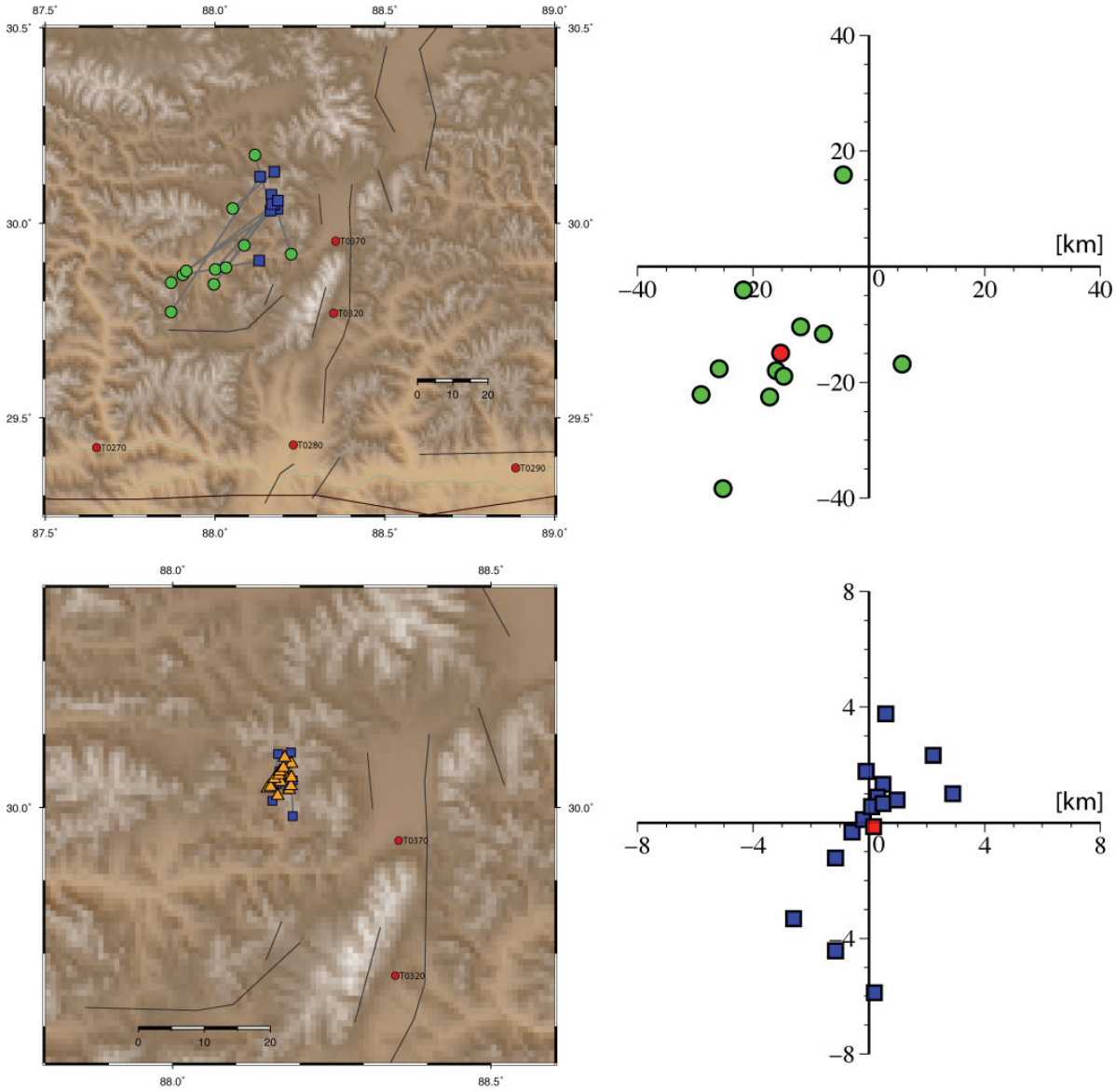

Figure 8. Comparison of NEIC (green circles), automatic Hi-CLIMB (blue squares), and manual Hi-CLIMB (orange triangles) earthquake locations for the PQX reveals (top) a general SW NEIC location bias that can reach more than 40 km (average value for 11 common events is 25 km) and (bottom) a close correspondence of locations based on automatic and manual P- and S-phase picks, respectively (average epicenter difference for 15 events is 2 km). The closest Hi-CLIMB station (red circles) is about 20 km east of the epicenters. Right shows (top) NEIC relative to automatic Hi-CLIMB location (at center), and (bottom) automatic relative to manual Hi-CLIMB location (at center). Red symbols are "centroid" shifts of ~20 km to the SW and ~0 km, respectively.

However, the manual hypocenter depths of ~10 km are consistent with shallow 6-9 km depths (with uncertainties probably on the order of ±3 km) from regional moment tensor analysis of 36 larger ($3.5 \leq M_w \leq 4.8$) earthquakes from modeling Hi-CLIMB data (Figure 9) (Baur, 2007; Monigle et al., 2009). This suggests that actual hypocenter resolution for events from July 2004 to August 2005, for which location and waveform modeling were performed, is close to GT5. All source mechanisms show ~N-S oriented normal faulting with a ~25-30º shallow west-dipping nodal plane. Solutions for events when sites east of 86º E were operating are highly consistent suggesting a small rupture area in agreement with the tight epicenter cluster from earthquake location.

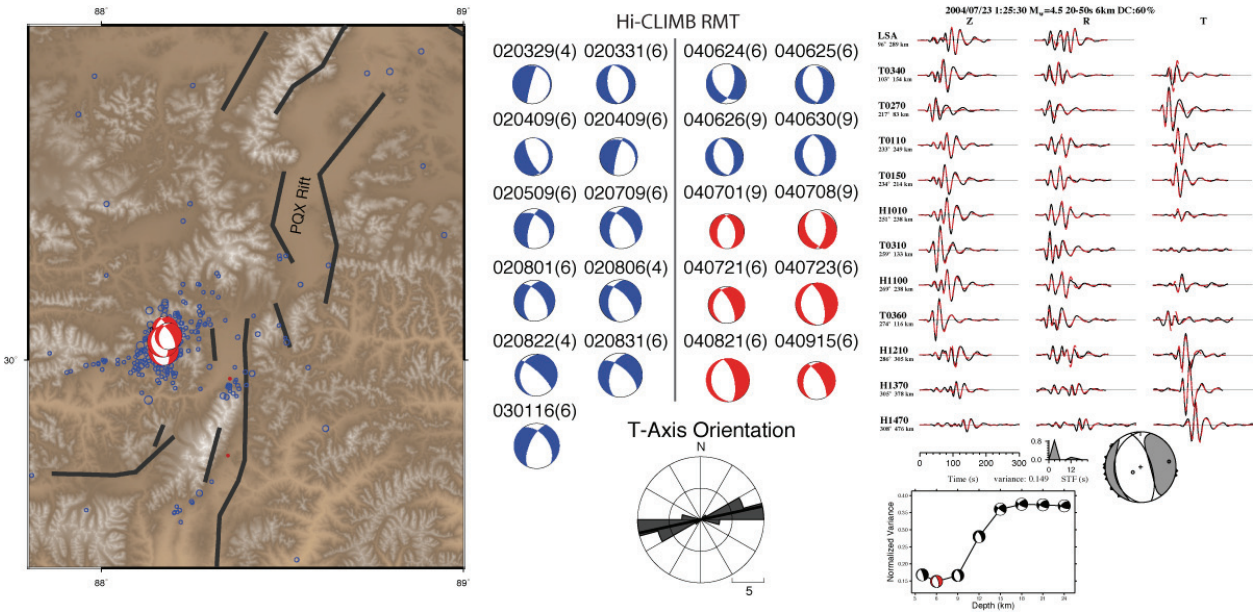

Figure 9. Left. Hi-CLIMB epicenters (blue) plotted with corresponding regional moment tensors (red) when close-by sites operated. Center. Selected fault plane solutions from regional moment tensor analysis. Red are best-constrained events in terms of location and moment tensor because of operating close-by sites; blue are events before local sites where installed. Right. Example of waveform fit (black observed, red synthetic, shown are only selected sites) for a M_w=4.5 event. All events are constrained by a large number of three-component waveforms from at least 20 stations. All solutions are consistent with shear faulting, are shallow, and indicate normal faulting along a N-S to NNW-SSE trending fault.

Based on event locations, source mechanisms, and Google imagery showing no prominent scarps in the immediate vicinity of the earthquakes, we favor a scenario of rupture along the eastern PQX rift boundary fault, a west-dipping low-angle normal fault and the most prominent feature on the Google imagery. The N-S extent of the cluster coincides with the dimensions (~20 km) of the basin, just east of the event-cluster, which forms a short, bounded rift segment. Combining the consistent observations leads to a preferred interpretation of active low-angle normal faulting. Physically, low-angle faulting is difficult to achieve unless the stress field is rotated or resolved shear stress is very low. Presence of fluids, likely in this geothermal region, could possibly achieve both. Globally, our study is one of the first to document possible low-angle faulting. Given uncertainties in location, depth, and dip and choice of nodal plane, other scenaria cannot be ruled out. The fault could be steeply east dipping or could have occurred on an unidentified west-dipping fault west of the PQX. Surface morphology, however, supports neither alternative.

Initial results were presented at the 2009 AGU meeting (Monigle et al., 2009). We are currently finalizing absolute and relative locations based on manual P- and S-phase picks for prominent events during the 2002-2005 sequence to test our initial interpretation.

CONCLUSIONS AND RECOMMENDATIONS

The Hi-CLIMB broadband seismic dataset provides the opportunity for ground truth location, source parameter determination and studying distance evolution of seismic coda in central Asia. The dataset reveals an abundance of seismic events not included in any other catalog. We developed modules to clean up the automatic event location database that eliminate spurious phase arrivals leading to improved locations, or, where this was impossible, remove spurious events entirely. The resulting database contains over 34,000 events with almost 9,000 based on 30 or more P and S arrivals. Initial M_L determination indicated systematic underestimation and frequent contamination of smaller events by later, larger events due to the high level of seismicity. Instead of determining M_L from S phases, we implemented a local magnitude based on P wave amplitudes $M_L(P)$ and use a simple, physics-based conversion to obtain regular M_L. We analyze the vigorous seismicity near the Pumqu-Xianza Rift for precise hypocenter locations and regional moment tensor determination to evaluate events for GT-locations. Knowledge gained from the small Pumqu-Xianza area will be transferred to GT-location determination and evaluation in other areas covered by the Hi-CLIMB array. The GT level locations and moment tensor depths will contribute to SLBM tomographic efforts, allow evaluation of depth for crustal models, and enhance model accuracy throughout central and southern Asia and, in general, will contribute to the National Nuclear Security Administration (NNSA) Knowledge Base.

REFERENCES

Baur, J. (2007). Seismotectonic analysis of the Himalayan-Tibetan collision zone from regional seismic moment tensor analysis with Hi-CLIMB data, *M.Sc. thesis, Oregon State University, Corvallis, Oregon*, 276 pp.

Bondar, I., S. C. Myers, E. R. Engdahl, E. A. Bergman (2004). Epicentre accuracy based on seismic network criteria, *Geophys. J. Int*. 156: 483–496, doi: 10.1111/j.1365-246X.2004.02070.x, 2004.

Braunmiller, J., N. Deichmann, D. Giardini, W. Wiemer, and the SED Magnitude Working Group (2005). Homogeneous moment-magnitude calibration in Switzerland, *Bull. Seis. Soc. Am.*, 95, 58-74, doi: 10.1785/0120030245.

Burtin, A. (2005). Seismotectonics of the Himalayan arc from regional seismogram moment tensor inversion, *Internship Report, Oregon State University, Corvallis, Oregon*, 42 pp.

Burtin, A., J. Nábělek, J. Baur, and J. Vergne (2005). Evidence for the decoupling of stress above and beneath the Main Himalayan Thrust, *Eos Trans. Am. Geophys. Union* 86: (52): Fall Meet. Suppl., Abstract T43A-1379.

Carpenter, S. (in prep. 2010). *M.Sc. thesis, Oregon State University, Corvallis, Oregon*.

De la Torre, T. L., G. Monsalve, A. F. Sheehan, S. Sapkota, and F. Wu (2007). Earthquake processes of the Himalayan collision zone in eastern Nepal and the southern Tibetan Plateau, *Geophys. J. Int.* 171: 718-738, doi: 10.1111/j.1365-246X.2007.03537.x

Monigle, P. W., J. Nábělek, J. Braunmiller, S. Carpenter, and J. R. Baur (2009). Earthquake activity along the Pumqu-Xianza rift (Tibet) and its tectonic implications, *Eos Trans. AGU*, 90(52), Fall Meet. Suppl., Abstract T43C-2111.

Nábělek, J. and G. Xia (1995). Moment-tensor analysis using regional data: application to the 25 March 1994 Scotts Mills, Oregon earthquake, *Geophys. Res. Lett*. 22: 1316.

Nábělek, J., J. Vergne, G. Hetenyi, and the Hi-CLIMB Team (2005). Project Hi-CLIMB: a synoptic view of the Himalayan collision zone and southern Tibet, *Eos Trans. Am. Geophys. Union* 86: (52): Fall Meet. Suppl., Abstract T52A-02.

Nábělek, J., G. Hetényi, J. Vergne, S. Sapkota, B. Kafle, M. Jiang, H. Su, J. Chen, B.-S. Huang, and the Hi-CLIMB Team (2009a). Underplating in the Himalaya-Tibet collision zone revealed by the Hi-CLIMB experiment, *Science* 325: 1371, doi: 10.1126/science.1167719.

Nábělek, J. L., J. Braunmiller, and W. Scott Phillips (2009b). Source and path calibration in regions of poor crustal propagation using temporary, large-aperture, high-resolution seismic arrays, in *Proceedings of the 2009 Monitoring Research Review: Ground-Based Nuclear Explosion Monitoring Technologies*, LA-UR-09-05276, Vol. 1, pp. 158-165.

Sheehan, A. F., G. Monsalve, C. Rowe, and M. Begnaud (2004). Ground truth in central Asia from in-country networks, in *Proceedings of the 26th Seismic Research Review: Trends in Nuclear Explosion Monitoring*, LA-UR-04-5801, Vol. 1, pp. 338–345.

Velasco, A. A., V. L. Gee, C. Rowe, D. Grujic, L. S. Hossister, D. Hernandez, K. C. Miller, T. Tobgay, M. Fort, and S. Harder (2007). Using small, temporary seismic networks for investigating tectonic deformation: Brittle deformation and evidence for strike-slip faulting in Bhutan, *Seis. Res. Lett.* 78: (4) 446-453, doi: 10.1785/gssrl.78.4.446.